2019

Degradation and Deactivation of Bacterial Antibiotic Resistance Genes during Exposure to Free Chlorine, Monochloramine, Chlorine Dioxide, Ozone, Ultraviolet Light, and Hydroxyl Radical

Huan He

Peiran Zhou

Kyle Shimabuku

Xuzhi Fang

Shu Li

See next page for additional authors

Authors

Huan He, Peiran Zhou, Kyle Shimabuku, Xuzhi Fang, Shu Li, Yunho Lee, and Michael C. Dodd

Environmental Science & Technology

Article

Cite This: Environ. Sci. Technol. 2019, 53, 2013−2026

pubs.acs.org/est

Degradation and Deactivation of Bacterial Antibiotic Resistance Genes during Exposure to Free Chlorine, Monochloramine, Chlorine Dioxide, Ozone, Ultraviolet Light, and Hydroxyl Radical

Huan He,[†] Peiran Zhou,[†,§] Kyle K. Shimabuku,[†,§] Xuzhi Fang,[†] Shu Li,[†] Yunho Lee,[‡] and Michael C. Dodd*[,†]

[†]Department of Civil and Environmental Engineering, University of Washington (UW), Seattle, Washington 98195-2700, United States

[‡]School of Earth Sciences and Environmental Engineering, Gwangju Institute of Science and Technology (GIST), Gwangju 61005, Republic of Korea

Supporting Information

ABSTRACT: This work investigated *degradation* (measured by qPCR) and biological *deactivation* (measured by culture-based natural transformation) of extra- and intracellular antibiotic resistance genes (eARGs and iARGs) by free available chlorine (FAC), NH_2Cl, O_3, ClO_2, and UV light (254 nm), and of eARGs by $^{\bullet}OH$, using a chromosomal ARG (*blt*) of multidrug-resistant *Bacillus subtilis* 1A189. Rate constants for *degradation* of four 266−1017 bp amplicons adjacent to or encompassing the *acfA* mutation enabling *blt* overexpression increased in proportion to #AT+GC bps/amplicon, or in proportion to #5′-GG-3′ or 5′-TT-3′ doublets/amplicon, with respective values ranging from 0.59 to 2.3 ($\times 10^{11}$ M^{-1} s^{-1}) for $^{\bullet}OH$, 1.8−6.9 ($\times 10^{4}$ M^{-1} s^{-1}) for O_3, 3.9−9.2 ($\times 10^{3}$ M^{-1} s^{-1}) for FAC, 0.35−1.2($\times 10^{1}$ M^{-1} s^{-1}) for ClO_2, and 2.0−8.8 ($\times 10^{-2}$ cm^2/mJ) for UV at pH 7, and from 1.7−4.4 M^{-1} s^{-1} for NH_2Cl at pH 8. For FAC, NH_2Cl, O_3, ClO_2, and UV, ARG *deactivation* paralleled *degradation* of amplicons approximating a ∼800−1000 bp *acfA*-flanking sequence required for natural transformation in *B. subtilis*, whereas *deactivation* outpaced *degradation* for $^{\bullet}OH$. At practical disinfectant exposures, eARGs and iARGs were ≥90% *degraded/deactivated* by FAC, O_3, and UV, but recalcitrant to NH_2Cl and ClO_2. iARG *degradation/deactivation* always lagged cell inactivation. These findings provide a quantitative framework for evaluating ARG fate during disinfection/oxidation, and support using qPCR as a proxy for tracking ARG *deactivation* under carefully selected circumstances.

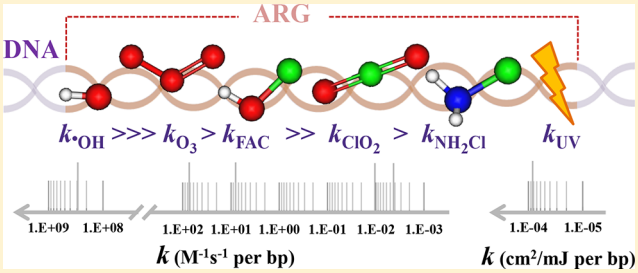

INTRODUCTION

The proliferation of antibiotic resistance since the early 20th century has decreased the therapeutic effectiveness of antibiotics,[1] leading to associated increasing mortality, morbidity, and economic losses worldwide.[2,3] Antibiotic resistant bacteria and resistance genes (ARB and ARGs) are now known to be widespread in aquatic environments. For example, ARBs and ARGs have been found in liquid animal wastes and manure derived from confined animal feed operations,[4,5] municipal wastewaters,[4,6−8] surface waters and associated sediments,[4,6,9] and drinking water treatment and distribution systems.[4,10,11]

In this context, (waste)water treatment could potentially provide an important barrier to ARB/ARG dissemination. (Waste)water disinfection processes may play a particularly critical role by inactivating ARB. However, even if ARB are fully inactivated during disinfection, intact DNA remnants within the resulting cell debris could possibly confer resistance to downstream bacterial populations via horizontal gene transfer (HGT). For example, through natural transformation, ARGs carried on extracellular plasmid or genomic DNA originating from a donor cell can be taken up by a "competent" nonresistant recipient cell, incorporated into the latter's genome, and expressed by the transformed recipient cell.[12,13] A wide variety of naturally competent strains have been identified,[13,14] including many important human pathogens.[15] In addition, while natural transformation is typically most facile among the same species, interspecies transformation is also possible.[13,16] Because extracellular DNA molecules may persist within aquatic systems over extended periods via adsorption onto or complexation with cellular debris, clay, sand, or humic constituents,[13,17,18] natural transformation could also mediate ARG transfer to bacterial populations temporally or spatially distant from donor cells.[13]

Previous studies have demonstrated that ARGs are degraded with widely varying efficiencies by disinfectants/oxidants

Received: August 7, 2018
Revised: November 23, 2018
Accepted: December 3, 2018
Published: February 3, 2019

DOI: 10.1021/acs.est.8b04393
Environ. Sci. Technol. 2019, 53, 2013−2026

Scheme 1. Procedures for Treatment of eARGs and iARGs with Each Disinfectant and Subsequent Analyses to Quantify ARG Degradation, ARG Deactivation, and ARB Inactivation

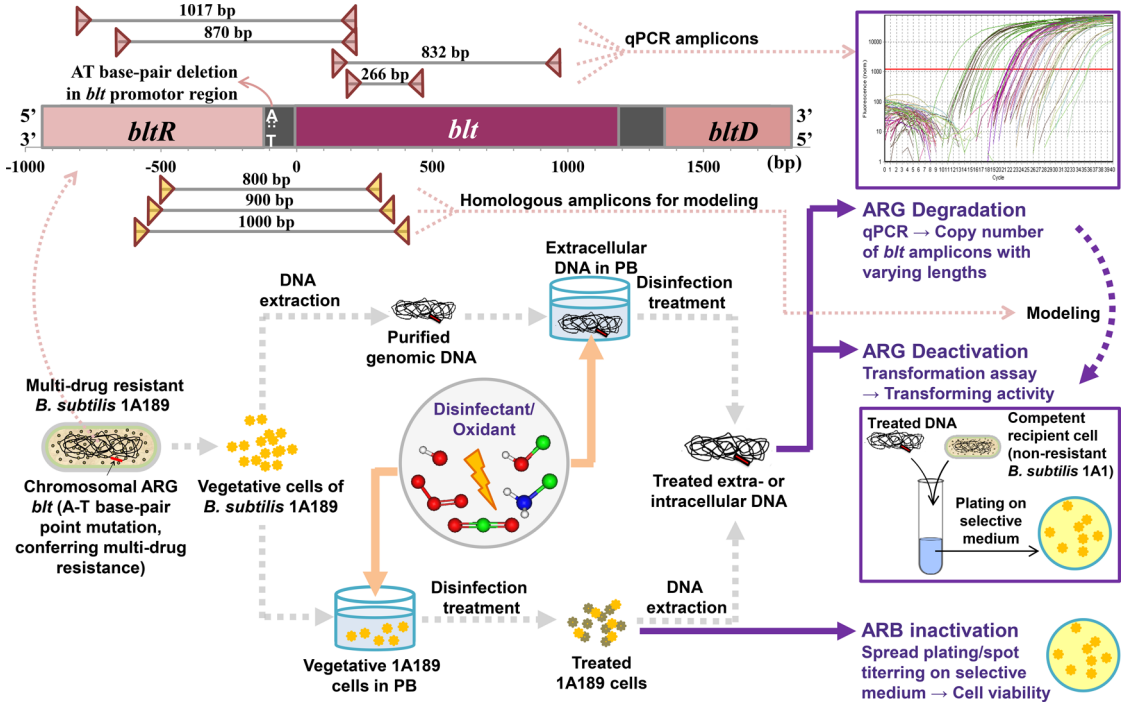

including free available chlorine (FAC),[19] monochloramine (NH_2Cl),[20,21] chlorine dioxide (ClO_2),[22] ozone (O_3),[23,24] ultraviolet (UV) light,[19,21,25−29] and hydroxyl radical ($^{\bullet}OH$).[19] However, few have elucidated the fundamental kinetic parameters governing ARG *degradation*,[19,24,27] making it difficult to compare prior results obtained under different experimental conditions. In addition, relatively few have investigated the impacts of disinfection processes on ARG biological activities,[27,60] in turn hindering assessment of the environmental/biological implications of ARG *degradation* during these processes. Furthermore, recent attention has focused primarily on reactions of disinfectants/oxidants with plasmid-borne ARGs[19,24,27] rather than chromosomal ARGs, even though natural transformation with chromosomal DNA is generally far more efficient than with plasmid DNA.[13]

This work was therefore undertaken to provide a comprehensive investigation of the fundamental kinetic parameters and mechanisms governing ARG *degradation* and *deactivation* by common (waste)water disinfectants/oxidants, including FAC, NH_2Cl, ClO_2, O_3, 254 nm UV light (hereafter simply UV), and $^{\bullet}OH$, using a model chromosomal ARG (*blt*) harbored by multidrug-resistant *Bacillus subtilis* strain 1A189. *blt* is a widely studied member of the major facilitator superfamily of multidrug transporters with broad substrate specificity, and a close homologue of the clinically relevant *norA* gene conferring fluoroquinolone resistance in *Staphylococcus aureus*.[30−32] *B. subtilis* was selected as a model bacterium on account of its ease of culturing and natural competence, widely available gene sequence data, and the relevance of it and related *Bacilli*—including pathogenic strains of *Streptococcus*, *Enterococcus*, and *Staphylococcus* spp., with which *B. subtilis* may exchange ARGs—as important members of soil, water, and human gastrointestinal microflora.[33]

The ability of each disinfectant to *degrade* and *deactivate* extracellular and intracellular ARGs was assessed by subjecting purified *B. subtilis* 1A189 DNA and intact *B. subtilis* 1A189 cells to increasing disinfectant exposures representative of (waste)water practice. A combination of culture-based and molecular microbiological techniques was used in parallel to monitor ARG *degradation* (i.e., decreases in ARG copy numbers measured by qPCR), ARG *deactivation* (i.e., elimination of ARG transforming activities), and donor ARB cell inactivation. *Degradation* kinetics were quantified for each disinfectant using a set of four 266−1017 bp amplicons with different nucleotide contents located adjacent to or encompassing the *acfA* mutation that enables *blt* overexpression in *B. subtilis* 1A189. Observed rate constants for the four amplicons were compared to their specific nucleotide contents to enable determination of fundamental *sequence-independent* rate constants for DNA reaction with each disinfectant. These fundamental kinetics parameters were in turn applied to predict the kinetics with which the DNA region responsible for *blt* transformation was *degraded* and *deactivated* during extra- and intracellular treatment by each disinfectant.

MATERIALS AND METHODS

Chemicals and Materials. All chemicals and growth media were purchased from commercial suppliers, certified-nuclease free, and of at least reagent-grade purity. Molecular biology grade water (Corning, NY) was utilized in DNA standard preparations, transformation assays and qPCR analyses. Milli-Q grade (≥18.2 MΩ cm) water was otherwise used to prepare chemical reagents and growth media, which (except disinfectants/oxidants and actinometry reagents) were then autoclaved or filter-sterilized prior to use. Preparations of aqueous stocks of FAC, NH_2Cl, ClO_2, O_3 and hydrogen peroxide (H_2O_2), as well as other reagents and culture media, are described in Supporting Information (SI) Text S1.

Bacterial Strains. *B. subtilis* strains 1A1 (nonresistant) and 1A189 (multidrug-resistant) were obtained from the Bacillus

DOI: 10.1021/acs.est.8b04393
Environ. Sci. Technol. 2019, 53, 2013−2026

Genetic Stock Center (BGSC; Ohio State University), revived, and cultured according to BGSC instructions. Genomic DNA of *B. subtilis* 1A189 exhibits a point mutation (*acfA* − an A-T base-pair deletion) in the promoter region of the 1203-bp wild-type *blt* gene, which is part of the *bltR-blt-bltD* genome segment characteristic of *B. subtilis*, as illustrated in Scheme 1. The mutant genome segment encodes constitutional efflux-mediated resistance to a wide variety of antibiotics (including fluoroquinolones, chloramphenicol, doxorubicin, and acriflavine), whereas the wild-type segment does not.[34]

DNA Extraction. High molecular weight DNA was isolated from *B. subtilis* 1A189 cells by phenol-chloroform-isoamyl alcohol extraction,[35] with additional purification steps. Detailed extraction procedures and recovery yields are provided in SI Text S2.

Natural Transformation Assay. Transforming activity of *B. subtilis* 1A189 DNA was quantified by natural transformation, using *B. subtilis* 1A1 as the recipient,[36,37] with key steps depicted in Scheme 1 and detailed protocols provided in SI Text S3. Transformation *frequency* was calculated as transformant cell density (CFU/mL) measured on selective media (with 4 mg/L acriflavine) over total recipient cell density (CFU/mL) on nonselective media (SI Text S4).

Quantitative Polymerase Chain Reaction (qPCR). qPCR assays were performed using an Eppendorf RealPlex^4 Mastercycler (Hauppauge, NY) with SsoFast EvaGreen Supermix[29] (Bio-Rad, Hercules, CA) to quantify gene copy numbers of 266−1017 bp *blt* amplicons. Primers were designed based on the *B. subtilis* 168 *bltR-blt-bltD* gene sequence (GenBank accession number: AL009126.3), and purchased from Eurofins (Huntsville, AL). The 266 and 832 bp amplicons target the *blt* gene, whereas the 870 and 1017 bp amplicons encompass the *acfA* mutation and span the *blt* promoter region between the *bltR* and *blt* genes (Scheme 1). Locations and sequences of the amplicons with corresponding primers are shown in SI Text S5. Their nucleotide contents, including numbers of interstrand AT, GC, and AT+GC base pairs (bps), and numbers of intrastrand 5′-GG-3′, and 5′-TT-3′doublets per amplicon, are summarized in SI Table S1. qPCR assay protocols (including amplification efficiencies, limits of detection and quantification (LODs & LOQs), etc.) are provided in SI Text S6.

Other DNA Analyses. DNA fragment sizes were analyzed by pulsed-field gel electrophoresis (PFGE) (SI Text S7). Double-stranded DNA (dsDNA) and monomeric deoxyribonucleoside 5′-monophosphate (dNMP, or nucleotide) concentrations were measured by (i) Hoechst 33258 fluorescence assay with a DNA Quantitation Kit (Bio-Rad) and (ii) nuclease P1 (Sigma) digestion followed by high performance liquid chromatography,[38] respectively.

Treatment of Extracellular ARGs (eARGs). *B. subtilis* 1A189 DNA was diluted and exposed to each disinfectant in autoclaved 10 mM phosphate buffer (PB) at pH 7 for FAC, ClO_2, O_3, UV, and $^{\bullet}OH$, and pH 8 for NH_2Cl to minimize NH_2Cl self-decomposition (see SI Text S8 for discussion of limited NH_2Cl experiments at pH 7), with FAC, NH_2Cl, ClO_2, and O_3 at ≥10-fold molar excess of DNA (as [dNMPs]). For FAC, NH_2Cl, and ClO_2, disinfection was performed in continuously stirred batch reactors by adding disinfectant stocks to 1 mg/L DNA solutions (3.2×10^{-6} M as total dNMPs). At predefined time intervals, reaction solutions were sampled and quenched with sodium thiosulfate ($Na_2S_2O_3$) (≥20-fold molar excess of [disinfectant]). For O_3, reactions were undertaken with 1 mg/L DNA solutions in the presence of 50 mM *tert*-butanol (*t*-BuOH) using a continuous-flow, quenched-reaction system (SI Text S8).[39] For UV, 1 mg/L DNA solutions contained in quartz tubes were irradiated with a low-pressure Hg lamp emitting monochromatic UV light at 254 nm in a "merry-go-round" photoreactor apparatus, and sampled at predefined times (SI Text S8). For $^{\bullet}OH$, 10 mg/L DNA solutions containing 10 mM H_2O_2 and 1 μM *para*-chlorobenzoic acid (*p*CBA, a $^{\bullet}OH$ probe) were irradiated with near-UV wavelengths (290−400 nm) to enable photolysis of H_2O_2 to $^{\bullet}OH$ while precluding DNA damage by direct photolysis (SI Text S8). At predefined times, samples were collected and residual H_2O_2 quenched with bovine liver catalase (Sigma; ≥ 10 units/μmole H_2O_2).

Residual disinfectant concentrations were monitored colorimetrically using DPD for FAC and NH_2Cl,[40] ABTS for ClO_2,[41] and indigo trisulfonate for O_3.[42] Fluence rates (*I*, in mW/cm^2) for UV irradiation experiments were quantified using atrazine,[43] iodide/iodate,[44] and/or ferrioxalate[44] actinometry. Pathlength was determined according to Zepp (1978),[45] using ferrioxalate actinometry.[44] Cumulative integrated exposures (or *CT* values) for chemical disinfectants were calculated as $\int_0^t [\text{Disinfectant}]dt$ (in mg/L·min or mol/L·s), whereas fluences (or *IT* values) for UV were calculated as $I \times t$ (in mJ/cm^2). $^{\bullet}OH$ exposures were determined by monitoring *p*CBA degradation in near-UV/H_2O_2 experiments.[46] Details of reactor configurations, additional experiments, disinfectant exposure measurements, actinometry procedures, and pathlength measurements are provided in SI Text S8.

Treatment of Intracellular ARGs (iARGs). Vegetative cells of *B. subtilis* 1A189 were dosed into autoclaved 10 mM PB solutions and exposed to each disinfectant at the same pH as in eARG treatment (*B. subtilis* intracellular pH has been reported to be ∼7.4 with an extracellular pH maintained at 6−8).[47] Disinfectant stocks were dosed to 1-L, 10^6-CFU/mL cell suspensions in batch reactors under stirring to yield 2 mg/L of FAC, NH_2Cl, or ClO_2, and 1 mg/L of O_3. O_3 experiments were performed with and without 50 mM *t*-BuOH ($^{\bullet}OH$ scavenger) to evaluate potential contributions of $^{\bullet}OH$ to iARG *degradation/deactivation* during ozonation. At predefined times, each 1-L reaction suspension was quenched with $Na_2S_2O_3$. For UV experiments, 100 mL volumes of a 10^6-CFU/mL cell suspension were each subdivided into four quartz tubes, irradiated for predefined times, and then recombined for subsequent analyses. Disinfectant exposures were determined as described above.

Treated cell viabilities were determined by direct spread-plating or spot-titering[48] of sample aliquots on selective media, with LODs permitting measurement of ∼5.5- or ∼5.1-$\log_{10}$ inactivation, respectively. Treated cells were recovered by vacuum filtration of full sample volumes through 0.2 μm track-etched polycarbonate membranes (Whatman, NJ) and processed for DNA extraction as described in SI Text S2. Intracellular DNA recovery was determined by measuring dsDNA concentration or dNMP concentrations if the former was below the fluorescence assay LOQ.

Scheme 1 provides an overview of the above experimental procedures. All experiments were performed in at least duplicate at 25 ± 1 °C (UV) or 20 ± 1 °C (other disinfectants). ARG transforming activities, ARG copy numbers, and DNA fragment sizes of collected DNA samples were analyzed as specified above. Normalized gene copy

DOI: 10.1021/acs.est.8b04393
Environ. Sci. Technol. 2019, 53, 2013−2026

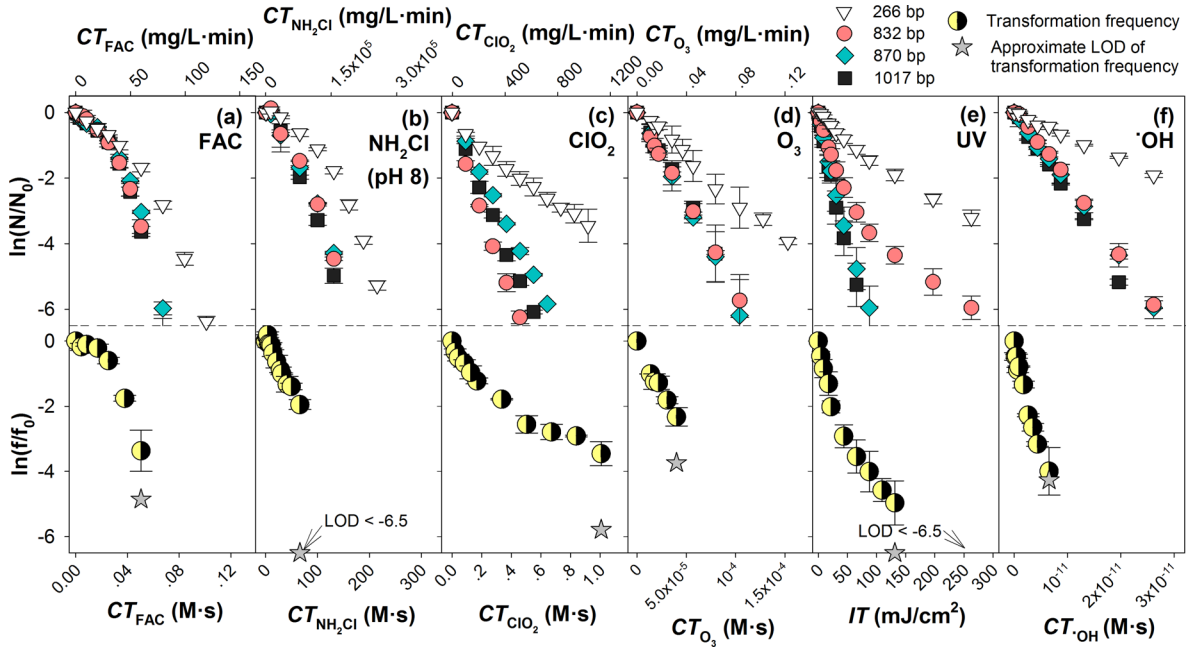

Figure 1. Normalized (natural log-scale) qPCR amplicon copy numbers (upper) and *blt* transformation frequencies (lower) versus *CT* values for (a) FAC, (b) NH_2Cl, (c) ClO_2, (d) O_3, and (f) $^{\bullet}OH$; and versus *IT* values for (e) UV. All data were obtained by treatment of extracellular *B. subtilis* 1A189 DNA in 10 mM phosphate buffer at pH 7 (FAC, ClO_2, O_3, $^{\bullet}OH$, and UV) or 8 (NH_2Cl only). LODs of normalized qPCR amplicon copy numbers were all below the lower *y*-axis limits (i.e., $\ln(N/N_0) < -6.5$), and are thus not shown, while LODs of normalized transformation frequencies are shown with star symbols for each disinfectant. Error bars represent one standard deviation from the mean, obtained from at least duplicate experiments conducted independently.

numbers (N/N_0) or normalized transformation frequencies (f/f_0) were calculated as gene copy number or transformation frequency of a given sample divided by that of a corresponding untreated control, respectively.

Statistical Analysis. Data from independent replicate experiments were pooled in order to perform least-squares linear regressions (using SigmaPlot 12.0) or nonlinear regressions (using Microsoft Excel SOLVER; SI Text S9) for determining first- or second-order rate constants (and associated uncertainties) of each *blt* amplicon in its reaction with each disinfectant. The method of weighted linear regression was applied to perform uncertainty-weighted regression analyses of first-order rate constants for each amplicon versus disinfectant concentrations, or for amplicon-specific second-order rate constants versus amplicon nucleotide contents, since the rate constants derived in each of these cases carry associated standard errors (since they are themselves obtained by linear regressions of measured data).[49] Here, for an *n*-number data set with *y*-direction standard errors, e_i, for each x_i, y_i pair (i.e., x_i, $y_i \pm e_i$), the individual weights (w_i) were defined as,

$$w_i = \frac{e_i^{-2}}{\sum_i e_i^{-2}/n} \tag{1}$$

The slope and intercept of the weighted regression line, their associated standard errors, and the coefficient of determination (R^2), were calculated as below,

$$\text{slope} = \frac{\sum_i w_i x_i y_i - n\bar{x}_w\bar{y}_w}{\sum_i w_i x_i^2 - n\bar{x}_w^2} \tag{2}$$

$$\text{intercept} = \bar{y}_w - \text{slope}\cdot\bar{x}_w \tag{3}$$

$$\text{slope\_error} = \frac{\sqrt{\sum_i w_i(y_i - y_{i,p})^2/(n-2)}}{\sqrt{\sum_i w_i(x_i - \bar{x}_w)^2}} \tag{4}$$

$$\text{intercept\_error} = \sqrt{\frac{\sum_i w_i(y_i - y_{i,p})^2}{n-2}}\cdot\sqrt{\frac{\sum_i w_i x_i^2}{n\sum_i w_i(x_i - \bar{x}_w)^2}} \tag{5}$$

$$R^2 = \frac{\left[\sum_i w_i(x_i - \bar{x}_w)(y_i - \bar{y}_w)\right]^2}{[\sum_i w_i(x_i - \bar{x}_w)^2]\cdot\left[\sum_i w_i(y_i - \bar{y}_w)^2\right]} \tag{6}$$

where $\bar{x}_w$ and $\bar{y}_w$ are the weighted mean values of x_i and y_i, which equal $\sum_i w_i x_i/n$ and $\sum_i w_i y_i/n$, respectively; and $y_{i,p}$ is predicted from the weighted regression line as slope·x_i + intercept. In this work, the weighted linear regressions were undertaken either by using Minitab 18 or by manually establishing eqs 1−6 in a Microsoft Excel spreadsheet, which have each been confirmed to yield consistent results.

Slopes of linear regressions obtained for data sets from selected UV experiments were compared using two-tailed *t*-tests with statistical significance defined as $p < 0.05$, and null hypothesis as no significant difference existing between slopes from the two data sets. Statistical analyses pertaining to determination of LODs and LOQs for qPCR assays are provided in SI Text S6.

RESULTS AND DISCUSSION

ARG Amplicon *Degradation*: Reaction Kinetics and Rate Constants. *Degradation* rates of the 266−1017 bp *blt* amplicons were monitored by employing qPCR to quantify damage to DNA sequences in the vicinity of the *acfA* point mutation responsible for *B. subtilis* 1A189 multidrug-resistance

DOI: 10.1021/acs.est.8b04393
Environ. Sci. Technol. 2019, 53, 2013−2026

Table 1. Summary of Kinetics Parameters (as Mean ± Standard Error) for ARG *Degradation* Measured in This Study

$k_{Disinfectant, Amp}$ [a]	266 bp	832 bp	870 bp	1017 bp	$k_{Disinfectant, Specific}$ [d]	$k_{Disinfectant, 0}$ [d]
$k_{FAC, Amp}$ [b] (M^{-1} s^{-1})	3.9(±0.3)×10^3	8.5 (±0.5)×10^3	8.1(±0.5)×10^3	9.2(±0.5)×10^3	7.2(±0.5) ((M AT+GC)$^{-1}$s^{-1})	2.1(±0.4)×10^3 (M^{-1} s^{-1})
$k_{FAC, N-Cl bp}$ [c] (M^{-1} s^{-1})	3.9(±0.2)×10^{-1}				NA	NA
$k_{NH_2Cl, Amp}$ [b] (M^{-1} s^{-1})	1.7(±0.1)	3.6(±0.1)	3.8(±0.2)	4.4(±0.2)	3.6(±0.1)×10^{-3} ((M AT+GC)$^{-1}$s^{-1})	6.9(±0.6)×10^{-1} (M^{-1} s^{-1})
$k_{NH_2Cl, N-Cl bp}$ [c] (M^{-1} s^{-1})	1.6(±0.1)×10^{-4}				NA	NA
$k_{ClO_2, Amp}$ (M^{-1} s^{-1})	3.5(±0.3)	1.2(±0.2)×10^1	8.9(±0.2)	1.2(±0.1)×10^1	2.6(±0.1)×10^{-1} ((M 5′-GG-3′)$^{-1}$s^{-1})	−8.1(±1.7)×10^{-1} (M^{-1} s^{-1})
$k_{O_3, Amp}$ (M^{-1} s^{-1})	1.8(±0.5)×10^4	6.1(±1.2)×10^4	5.3(±0.8)×10^4	6.9(±0.8)×10^4	6.5(±0.7)×10^1 ((M AT+GC)$^{-1}$s^{-1})	0.5(±4.5)×10^3 (M^{-1} s^{-1})
$k_{UV, Amp}$ (cm^2/mJ)	2.0(±0.1)×10^{-2}	5.2(±0.2)×10^{-2}	7.8(±0.4)×10^{-2}	8.8(±0.4)×10^{-2}	2.8(±0.3)×10^{-4} ((M 5′-TT-3′/M amplicon)$^{-1}$ (cm^2/mJ))	5.0(±3.3)×10^{-3} (cm^2/mJ)
$k_{\cdot OH, Amp}$ (M^{-1} s^{-1})	5.9(±0.8)×10^{10}	1.9(±0.2)×10^{11}	2.0(±0.2)×10^{11}	2.3(±0.3)×10^{11}	2.3(±0.1)×10^8 ((M AT+GC)$^{-1}$s^{-1})	−1.4(±2.2)×10^9 (M^{-1} s^{-1})

[a]All data were obtained by treatment of extracellular *B. subtilis* 1A189 DNA in 10 mM phosphate buffer at pH 7 (FAC, ClO_2, O_3, $^{\bullet}OH$, and UV) or 8 (NH_2Cl only). Significands of standard errors of $k_{Disinfectant, Amp}$ were rounded up to 0.1 if below 0.1. [b]Rate constant for the first step in the sequential reaction, i.e., reversible N-chlorination of amplicons (see SI eqs S1 and S6 for FAC and NH_2Cl, respectively). [c]Rate constant for the second step in the sequential reaction, i.e., irreversible C-chlorination of N-chlorinated amplicons—assumed to represent an "average" value per N-chlorinated bp, and to be the same for N-chlorinated bps in all four amplicons (see SI eqs S4 and S8 for FAC and NH_2Cl, respectively). [d]For each disinfectant, $k_{Disinfectant, Specific}$ and $k_{Disinfectant, 0}$ are, respectively, the slope and intercept of the correlations obtained by linear regression of the rate constants, $k_{Disinfectant, Amp}$, for the four amplicons versus corresponding specific nucleotide contents (Figure 2). $k_{Disinfectant, Specific}$ represents the *sequence-independent*, bp- or doublet-specific rate constant for each disinfectant, and $k_{Disinfectant, 0}$ is attributed to factors influencing DNA reactivity (e.g., secondary targets, specific sequence elements) that are not fully accounted for by eq 9 (see further discussion in SI Text S11). Significands of standard errors of $k_{Disinfectant, Specific}$ were rounded up to 0.1 if below 0.1.

during treatment of eARGs with each disinfectant. Previous work has confirmed that various types of DNA lesions—for example, 5′-TT-3′ cyclobutane pyrimidine dimers (TT-CPDs, the primary UV-induced lesions), 8-oxo-7,8-dihydro-2′-deoxyadenosine (8-oxoA) sites, and abasic sites—can block or greatly hinder *Taq* polymerase (utilized in the qPCR assays here) from reading along a stretch of dsDNA.[50,51] Although it has been reported that certain lesions (e.g., a single 8-oxo-7,8-dihydro-2′-deoxyguanosine, or 8-oxoG, site) can be bypassed by the *Taq* polymerase, and are thus effectively nondetectable by qPCR,[51] such lesions would most likely also be bypassed or even repaired by *B. subtilis* polymerases.[52] Thus, detectable losses in qPCR signal were tentatively taken to correspond to the introduction of one or more biologically relevant lesions, which would also block native *B. subtilis* polymerases, in the population of targeted amplicons within a given sample. Plots of $\ln(N/N_0)$ of the four amplicons versus *CT* or *IT* (to normalize for differences in disinfectant/oxidant concentrations and experimental timeframes) are presented for each disinfectant in Figure 1.

For FAC and NH_2Cl, amplicon *degradation* rates were observed to accelerate with increasing *CT* values for all four amplicons (Figure 1a,b). To explain these trends, it is hypothesized that FAC and NH_2Cl react with DNA in a sequential reaction pathway, with two steps, each following second-order kinetics: (i) initial N-chlorination at an amino group of a nucleotide (reversible by $Na_2S_2O_3$, and hence, not directly detectable by qPCR), characterized by the rate constant $k_{FAC, Amp}$ or $k_{NH_2Cl, Amp}$, and leading to organochloramine formation, H-bond disruption, and exposure of the nucleotide and its pairing partner toward subsequent attack by FAC or NH_2Cl, followed by (ii) irreversible C-chlorination at a carbon of one of the non-H-bonded nucleotides of an N-chlorinated nucleotide base pair (N−Cl bp), characterized by the rate constant $k_{FAC, N-Cl bp}$ or $k_{NH_2Cl, N-Cl bp}$, and leading to formation of stable halogenated products (with 5-chloro- and 8-chloro-derivatives likely prevailing for pyrimidines and purines, respectively),[53,54] and blockage of amplification during qPCR. Further discussion on the complex kinetics of FAC and NH_2Cl, as well as determination of $k_{FAC, Amp}$, $k_{FAC, N-Cl bp}$, $k_{NH_2Cl, Amp}$, and $k_{NH_2Cl, N-Cl bp}$, is provided in SI Text S9 and Figures S3−S11.

$\ln(N/N_0)$ was *linearly* related to *CT* or *IT* for the four amplicons during treatment with ClO_2, O_3, UV, and $^{\bullet}OH$ (Figure 1c−f), indicating that amplicon *degradation* by these disinfectants followed second-order or fluence-based first-order kinetics, according to eqs 7 or 8, respectively.

$$\ln(N/N_0) = -k_{Disinfectant, Amp}\int_0^t [\text{disinfectant}]dt = -k_{Disinfectant, Amp}CT \quad (7)$$

$$\ln(N/N_0) = -k_{Disinfectant, Amp}(I \times t) = -k_{Disinfectant, Amp}IT \quad (8)$$

Determinations of the rate constants $k_{Disinfectant, Amp}$ for ClO_2, O_3, UV and $^{\bullet}OH$ from linear regression of the data are presented in SI Figures S12−S15, respectively. Note that linear regressions of UV data were performed only up to 45 mJ/cm^2 to exclude moderate tailing in the data at higher *IT*s (potentially due to CPD photoreversal,[55] as discussed later).

The measured values of $k_{Disinfectant, Amp}$ for *degradation* of the four amplicons by each disinfectant are summarized in Table 1, and compared with available literature values in SI Table S3. For a given amplicon, the DNA reactivity toward the chemical disinfectants declines in the order $^{\bullet}OH \gg O_3 >$ FAC $\gg ClO_2 >$ NH_2Cl. The measurements of $k_{O_3, Amp}$ and $k_{UV, Amp}$ both agree well with literature values,[19,24,27] while the measured

DOI: 10.1021/acs.est.8b04393
Environ. Sci. Technol. 2019, 53, 2013−2026

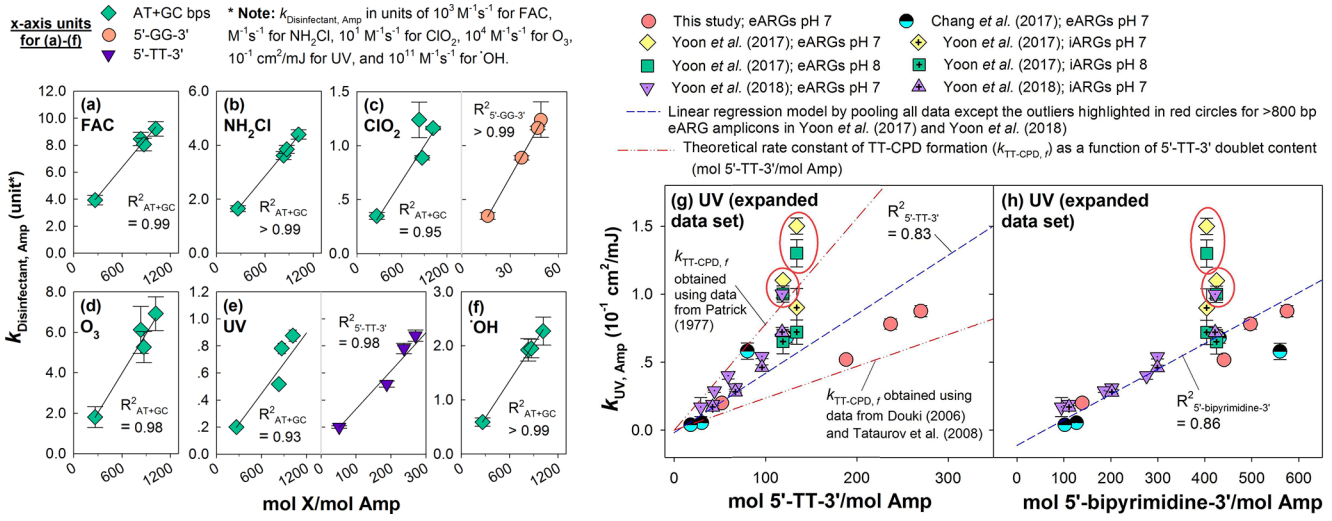

Figure 2. Second-order rate constants for (a) FAC, (b) NH_2Cl, (c) ClO_2, (d) O_3, and (f) $^{\bullet}OH$, and fluence-based first-order rate constants for (e) UV, plotted versus molar contents of nucleotide bps or specific doublets for 266 bp, 832 bp, 870 bp, and 1017 bp amplicons. All data were obtained by treatment of extracellular *B. subtilis* 1A189 DNA in 10 mM phosphate buffer at pH 7 (FAC, ClO_2, O_3, $^{\bullet}OH$, and UV) or 8 (NH_2Cl only). Panels (g) and (h) depict weighted linear regressions of UV data from this study, combined with data from prior studies by Chang et al. (2017),[27] Yoon et al. (2017),[19] and Yoon et al. (2018),[60] as well as theoretical rate constants, $k_{TT\text{-}CPD, f}$, of TT-CPD formation (panel (g) only) as a function of mol 5′-TT-3′/mol Amp calculated using data either from Patrick (1977),[61] or from Douki (2006)[62] and Tataurov et al. (2008),[63] according to the method of Yoon et al. (2018)[60] (see SI Text S12 for details). Regressions in (g) and (h) were performed without $k_{UV, Amp}$ measurements obtained for >800 bp eARG amplicons from the works by Yoon et al. (indicated by red circles), as these latter measurements may have been influenced by incidental photochemical generation of radicals from trace transition metals remaining in DNA extracts.[60] The values of the rate constants from the three prior works and the theoretical rate constants of TT-CPD formation for *blt* 266−1017 bp amplicons can be found in SI Table S3. Error bars represent standard errors from the mean for values determined in this work (Table 1) and either standard deviations or 95% confidence intervals from the mean as specified in the prior studies (SI Table S3). Trendlines and R^2 in panels (a)−(h) were obtained by weighted linear regressions of $k_{Disinfectant, Amp}$ versus specific nucleotide contents.

$k_{FAC, Amp}$ values (for initial N-chlorination by FAC) are >10× higher than those reported by Yoon et al. for 806−850 bp amplicons on the pUC4K plasmid.[19] Although it cannot be ruled out that this is due to inherent differences in plasmid and genomic DNA reactivities, it is worth noting that the prior values were determined according to an assumption of pseudo-first-order kinetics rather than the sequential-reaction model here. The $k_{^{\bullet}OH, Amp}$ values determined here are ∼10× higher than measurements by Yoon et al.[19] for plasmid-borne ARGs, but agree well with estimates of theoretical diffusion-controlled rate constants for polymeric (linear or supercoiled) DNA (SI Text S10).

Several prior investigators have also reported rate constants for reactions of DNA with FAC, O_3, and $^{\bullet}OH$ in terms of [dNMPs]; namely, ∼10 $(M\ dNMP)^{-1}s^{-1}$ for FAC (an estimated value specifically for dsDNA *denaturation* by FAC),[56] 410 $(M\ dNMP)^{-1}s^{-1}$ for O_3,[57] and 1.1−4.6(×10^8) $(M\ dNMP)^{-1}s^{-1}$ for $^{\bullet}OH$.[57−59] If the values of $k_{FAC, Amp}$, $k_{O_3, Amp}$, and $k_{^{\bullet}OH, Amp}$ measured here are each normalized to [dNMPs] (i.e., by dividing $k_{Disinfectant, Amp}$ by the total number of dNMPs—or twice the number of AT+GC bps—in each amplicon), they yield values ranging from 4.5 to 7.4 $(M\ dNMP)^{-1}s^{-1}$, 30−36 $(M\ dNMP)^{-1}s^{-1}$, and 1.1−1.2(×10^8) $(M\ dNMP)^{-1}s^{-1}$, respectively. While the dNMP-normalized values for FAC and $^{\bullet}OH$ agree well with the prior measurements, the reason for the differences for O_3 is uncertain. Several possibilities are that the presence of impurities within or partial denaturation of the calf thymus DNA utilized within the prior work (which was conducted under pseudo-first-order conditions, with DNA in excess of O_3) could have resulted in adventitious acceleration of O_3 decomposition (and over-estimation of k_{O_3}), or that the qPCR analyses utilized here did not capture all DNA lesions generated by reaction with O_3 (e.g., 8-oxoG). Investigation of these possibilities is recommended for future work.

With respect to the FAC rate constants determined here (Table 1), it is important to note that under various conditions, the kinetics of FAC reactions with organic molecules can be driven in part by chlorine species other than HOCl and OCl^-, namely Cl_2 and Cl_2O, where Cl_2 becomes more important at higher $[Cl^-]$ and lower pH, while Cl_2O becomes more important at higher [HOCl].[69,70] In cases for which Cl_2O contributions to observed reaction kinetics are important, deviations from first-order dependences on [FAC] can be expected, on account of the second-order dependence of Cl_2O formation on [HOCl].[69,70] As the FAC kinetics measurements obtained here indicated a clear first-order dependence on [FAC] (SI Text S9, Figure S9), it seems unlikely that Cl_2O contributed significantly to the observed rates of qPCR amplicon degradation. With regard to possible Cl_2 contributions—under the conditions used here, $[Cl^-]$ levels should not have exceeded 1−2 mM (due primarily to background Cl^- from the saline citrate used in preparing DNA stock solutions). Prior work suggests that under similar conditions (pH 7, 1 mM Cl^-), Cl_2 is unlikely to contribute to more than ∼10% of the observed degradation of aromatic compounds with measured rate constants, k_{HOCl}, of greater than ∼600 M^{-1} s^{-1} during treatment with FAC.[70] As values of $k_{FAC, Amp}$ were all in excess of 10^3 M^{-1} s^{-1}, it seems unlikely that Cl_2 could have contributed significantly to the proposed initial step of DNA chlorination (N-chlorination and H-bond disruption). However, a contribution of Cl_2 to the proposed

DOI: 10.1021/acs.est.8b04393
Environ. Sci. Technol. 2019, 53, 2013−2026

slower second step of DNA chlorination (irreversible nucleotide halogenation) cannot be ruled out on the basis of the available data. Although this does not alter the conclusions reached here, it is an important possibility that should be investigated in future work on DNA reactions with FAC.

ARG Amplicon *Degradation*: Influence of Amplicon Length and Nucleotide Content. Variations in $k_{\text{Disinfectant, Amp}}$ with amplicon composition were investigated by comparing measured $k_{\text{Disinfectant, Amp}}$ values with the length and nucleotide content of each amplicon, in order to determine whether consistent, predictable dependences of the magnitudes of $k_{\text{Disinfectant, Amp}}$ values on DNA sequence content could be identified. For each disinfectant, $k_{\text{Disinfectant, Amp}}$ generally increased in proportion to amplicon length (AT+GC bps), indicating that a larger number of nucleotides per amplicon results in a higher probability of an amplicon sustaining damage that prevents qPCR amplification (Figure 2a–f). Weighted linear regressions showed strong linear relationships of $k_{\text{Disinfectant, Amp}}$ with numbers of AT+GC bps per amplicon ($R^2 \geq 0.98$) for FAC, NH_2Cl, O_3, and $^{\bullet}OH$ (Figure 2a,b,d,f), while weaker relationships ($R^2 \leq 0.95$) were observed for ClO_2 and UV (Figure 2c, e).

The strengths of the regressions for FAC, NH_2Cl, O_3, and $^{\bullet}OH$ suggest that their reactivities toward a given amplicon depend on both the AT and GC bp content of the amplicon. While no prior measurements of NH_2Cl-nucleobase kinetics appear to be available for comparison, these trends are consistent with prior observations that FAC and O_3 react relatively rapidly ($k \sim 10^3$–10^4 M^{-1} s^{-1}) with both thymine and guanine nucleotides,[56,57] and that $^{\bullet}OH$ exhibits very high, nonselective reactivity ($k \sim 10^9$–10^{10} M^{-1} s^{-1}) toward all nucleobases.[64,65] The relatively weaker relationships of $k_{\text{Disinfectant, Amp}}$ with AT+GC bp content observed for ClO_2 and UV suggest that their reactivities toward a given amplicon likely depend more specifically on either AT or GC bp contents, or on the content(s) of some other sequence element(s) (e.g., nucleotide doublets or triplets) not captured by more general correlations of $k_{\text{Disinfectant, Amp}}$ with amplicon length.

This latter possibility was evaluated by undertaking additional weighted linear regressions of $k_{\text{ClO}_2\text{, Amp}}$ and $k_{\text{UV, Amp}}$ versus numbers of interstrand AT bps, GC bps, and all possible intrastrand nucleotide doublet and triplet permutations within each amplicon (regression parameters and statistics are summarized in SI part D). $k_{\text{ClO}_2\text{, Amp}}$ was indeed found to correlate much more strongly with intrastrand 5′-GG-3′ doublet content ($R^2_{\text{5′-GG-3′}} > 0.99$) in each amplicon (Figure 2c). This observation is in agreement with prior findings that guanine is the most susceptible nucleobase in dsDNA toward one-electron oxidants such as ClO_2 ($k_{\text{ClO}_2\text{, 5′-GMP}} = 4.5 \times 10^2$ M^{-1} s^{-1} at pH 7),[66] and that one-electron oxidation reactions preferentially lead to damage at the 5′-guanine of 5′-GG-3′ doublets.[67] (Note that the counts of intrastrand 5′-GG-3′ doublets used in SI part D for correlations exclude those within 5′-GGG-3′ or 5′-GGGG-3′ sequences (SI Table S1), which have been reported to react by single-electron transfer ~5–9× slower than isolated 5′-GG-3′ doublets at pH 7.0.[68])

$k_{\text{UV, Amp}}$ was likewise found to correlate much more strongly with intrastrand 5′-TT-3′ doublet content ($R^2_{\text{5′-TT-3′}} = 0.98$) (Figure 2e). This result agrees with previous findings,[19,27–29,60] and can be explained by the tendency of UV to generate lesions at intrastrand 5′-bipyrimidine-3′ sites, with 5′-TT-3′ more susceptible than 5′-TC-3′, 5′-CT-3′ and 5′-CC-3′ ($R^2_{\text{5′-TC-3′}} = 0.96$, $R^2_{\text{5′-CT-3′}} = 0.95$, and $R^2_{\text{5′-CC-3′}} = 0.71$; SI part D).[29,62] Although DNA can also sustain damage at 5′-TC-3′, 5′-CT-3′, and 5′-CC-3′, model predictions of the relative photoreactivities of each of the four 5′-bipyrimidine-3′ doublets indicate that TT-CPDs are likely to account for the majority of UV-induced lesions in the 266–1017 bp amplicons under the conditions applied here (SI Text S12). Consistent with this, $k_{\text{UV, Amp}}$ values measured for the 266–1017 bp amplicons are within the ranges of theoretical rate constants, $k_{\text{TT-CPD, }f}$, for TT-CPD formation in each amplicon, calculated as described in SI Text S12 (Figure 2g, SI Table S3).

Values of $k_{\text{UV, Amp}}$ from three recent studies investigating various plasmid-borne ARGs[19,27,60] are also shown in Figure 2g for comparison with the values measured here. These data indicate that the values from all four studies correlate with 5′-TT-3′ content, though considerable spread is apparent in the trends, with the plasmid-borne amplicons from the prior studies appearing to exhibit higher photoreactivities per unit of molar 5′-TT-3′ content than the chromosomal 266–1017 bp amplicons investigated here. While the possibility of inherent differences in chromosomal vs plasmid-borne amplicon photoreactivities cannot be excluded, it should be noted that these differences may instead arise from wide variations in the amplicons' proportions of 5′-TT-3′ doublets relative to their total 5′-bipyrimidine-3′ doublet contents $\left(f_{\frac{\text{5′-TT-3′}}{\text{5-bipyrimidine-3′}}} = \frac{\text{\#5′-TT-3′}}{\text{\#5′-TT-3′ + \#5′-TC-3′ + \#5′-CT-3′ + \#5′-CC-3′}}\right)$. Compared to the 266–1017 bp amplicons, the amplicons from the previous three studies are significantly more enriched in GC bps relative to AT bps, and are thus also more enriched in 5′-TC-3′, 5′-CT-3′, and 5′-CC-3′ doublets relative to 5′-TT-3′, with $f_{\frac{\text{5′-TT-3′}}{\text{5-bipyrimidine-3′}}}$ varying from 0.14–0.29 for the Chang et al. (2017)[27] data set and 0.21–0.38 for the Yoon et al. (2017, 2018)[19,60] data sets, compared to 0.37–0.48 for the 266–1017 bp amplicons investigated in this work. Consequently, the simple correlation of $k_{\text{UV, Amp}}$ with 5′-TT-3′ – which works very well for the 266–1017 bp amplicons – may not fully account for the role of the 5′-TC-3′, 5′-CT-3′, and 5′-CC-3′ doublets in governing photoreactivities of the amplicons from the prior works. This is supported by the stronger aggregate correlation of the $k_{\text{UV, Amp}}$ values from all four studies with overall molar 5′-bipyrimidine-3′ content (Figure 2h). In accord with these observations, Figure S16 and the discussion in Text S12 show that theoretical rate constants for TT-CPD formation, $k_{\text{TT-CPD, }f}$, cannot reconcile the differences in $k_{\text{UV, Amp}}$ values of the amplicons investigated across all four studies, whereas theoretical predictions of rate constants for *overall* bipyrimidine lesion formation, $k_{\text{all lesions, }f}$ (based on data from Douki (2006)[62] and Tataurov (2008)[63]), align well with the measured values of $k_{\text{UV, Amp}}$ across the whole set of amplicons (aside from the apparent outliers noted from the Yoon et al. studies[19,60]). This suggests that for ARGs that are significantly more enriched in GC bps than the *bltR-blt-bltD* genome segment investigated here, it may be important to account for the photoreactivities not only of 5′-TT-3′, but also of 5′-TC-3′, 5′-CT-3′, and 5′-CC-3′.

Interestingly, as shown in SI part D, correlations between $k_{\text{Disinfectant, Amp}}$ and various nucleotide bps, doublets, or triplets for FAC, NH_2Cl, O_3, and $^{\bullet}OH$ indicated that each of these oxidants may also exhibit preferential reactivities toward

DOI: 10.1021/acs.est.8b04393
Environ. Sci. Technol. 2019, 53, 2013–2026

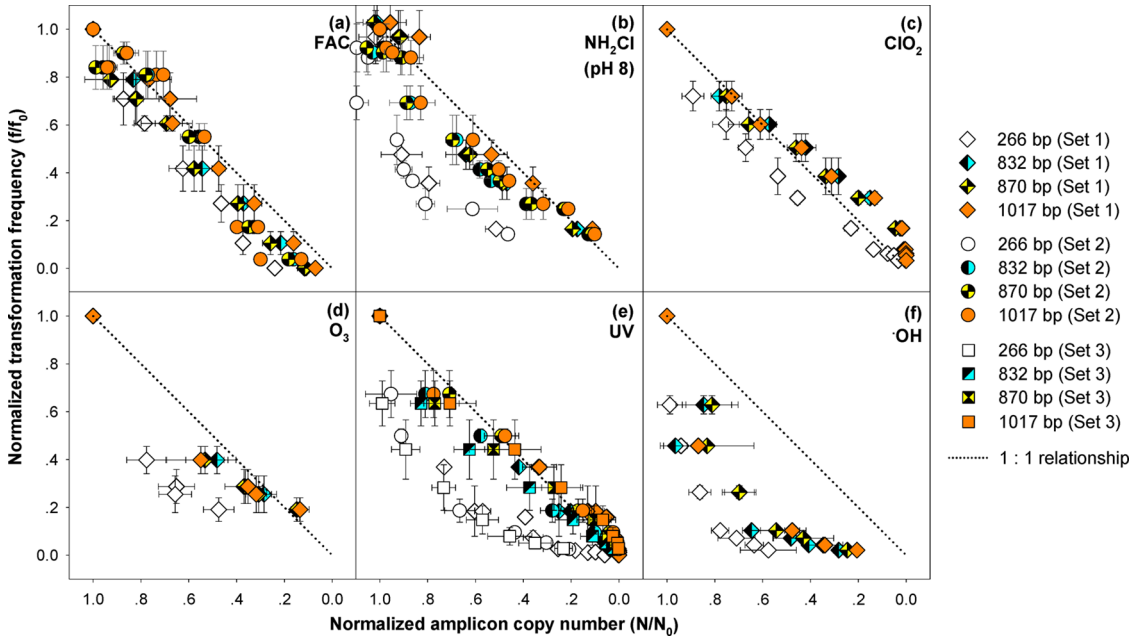

Figure 3. Normalized transformation frequency (f/f_0) plotted versus normalized copy number (N/N_0) of 266 bp, 832 bp, 870 bp, and 1017 bp amplicons for eARG treatment with (a) FAC, (b) NH_2Cl, (c) ClO_2, (d) O_3, (e) UV, and (f) $^{\bullet}OH$. All data were obtained by treatment of extracellular *B. subtilis* 1A189 DNA in 10 mM phosphate buffer at pH 7 (FAC, ClO_2, O_3, $^{\bullet}OH$, and UV) or 8 (NH_2Cl only). The *CT*s used for NH_2Cl and ClO_2 were much greater than *CT*s typically applied in practice. The narrow range of O_3 data is attributable to the inability to collect samples at lower exposure ranges using the continuous flow, quenched-reaction method (SI Text S8), on account of the very rapid kinetics of the O_3-DNA reaction. Sets 1, 2, and 3 (plotted using different symbol shapes) represent independent experiments undertaken under the same conditions but on different dates, each in at least duplicate. Error bars represent one standard deviation from the mean, obtained from at least duplicate experiments conducted independently on the same date. The dotted lines represent theoretical 1:1 relationships, as opposed to regression lines.

specific target sites within a given DNA sequence (e.g., FAC for GC bps and/or 5′-GT-3′ doublets, NH_2Cl for AT bps and 5′-AG-3′ doublets, O_3 for GC bps and 5′-GT-3′ doublets, and $^{\bullet}OH$ for 5′-TG-3′ doublets). Although more extensive evidence is needed to confirm the preferential occurrence of reactions at these sites (as has been demonstrated for attack of 5′-GG-3′ and 5-TT-3′ doublets by ClO_2 and UV),[62,67,68] these correlations may prove useful in guiding identification of reactive sites in future work.

The strong linear relationships of $k_{\text{Disinfectant, Amp}}$ with AT +GC bps for FAC, NH_2Cl, O_3, and $^{\bullet}OH$; 5′-GG-3′ doublets for ClO_2; and 5′-TT-3′ doublets for UV suggest that the reactivity of a given DNA segment toward each disinfectant can be predicted using a model such as eq 9,

$$k_{\text{Disinfectant, Amp}} = k_{\text{Disinfectant, Specific}}\cdot(\text{mol X/mol Amp}) + k_{\text{Disinfectant, 0}} \quad (9)$$

where $k_{\text{Disinfectant, Specific}}$ and $k_{\text{Disinfectant, 0}}$ are the respective slopes and intercepts of the corresponding regression lines in Figure 2a–f. $k_{\text{Disinfectant, Specific}}$ represents the rate constant for a given disinfectant normalized to nucleotide *bps* or *doublets* of type X (where X = AT+GC bps for FAC, NH_2Cl, O_3, and $^{\bullet}OH$; 5′-GG-3′ doublets for ClO_2; and 5′-TT-3′ doublets for UV), and $k_{\text{Disinfectant, 0}}$ is attributed to factors influencing DNA reactivity (e.g., secondary targets, specific sequence elements) that are not fully accounted for in the relatively simple single-parameter model represented by eq 9 (see further discussion in SI Text S11). The resulting $k_{\text{Disinfectant, Specific}}$ and $k_{\text{Disinfectant, 0}}$ values are summarized in Table 1.

Relationship of ARG Transforming Activity to qPCR Signals. While qPCR is a rapid, widely accessible, and affordable analytical tool to quantify damage within a DNA segment, direct measurement of changes in biological activity via culture-based transformation assay represents a "gold standard" approach for evaluating the impact of treatment processes on ARG dissemination risk.[27,71] In order to ascertain whether one measurement can be directly related to the other, changes in qPCR measurements for each of the investigated amplicons were compared with changes in measurements of residual transforming activities during exposure of *B. subtilis* 1A189 DNA to each disinfectant. As shown in Figure 1a–e, for FAC, NH_2Cl, ClO_2, O_3, and UV, ARG *deactivation* kinetics were significantly faster than for 266 bp amplicon *degradation*, but generally close to 832 bp, 870 bp, and/or 1017 bp amplicon *degradation* kinetics over the monitored exposure ranges (except for ClO_2 at CT_{ClO2} > ~0.2 M·s and UV at *IT* > ~45 mJ/cm^2). Figure 3 depicts measurements of residual transforming activity versus residual amplicon copy number (each normalized to untreated controls) during treatment with each disinfectant. For FAC, NH_2Cl, ClO_2, O_3, and UV, Figure 3a–e clearly illustrates that the 266 bp amplicon underestimates damage as measured by the transformation assay, while the 832–1017 bp amplicons generally capture damage at similar (~1:1) rates as the transformation assay (except at >70% or >90% *deactivation* by ClO_2 or UV, respectively). Results observed for NH_2Cl at pH 7 were consistent with those at pH 8 (SI Figure S17). In contrast, for $^{\bullet}OH$ treatment, ARG *deactivation* greatly outpaced *degradation* of all four amplicons (Figures 1f and 3f).

The above relationships between ARG *degradation* and *deactivation* can be understood in light of DNA integrity requirements for bacterial natural transformation driven by homologous recombination. Prior studies have reported that a

DOI: 10.1021/acs.est.8b04393
Environ. Sci. Technol. 2019, 53, 2013–2026

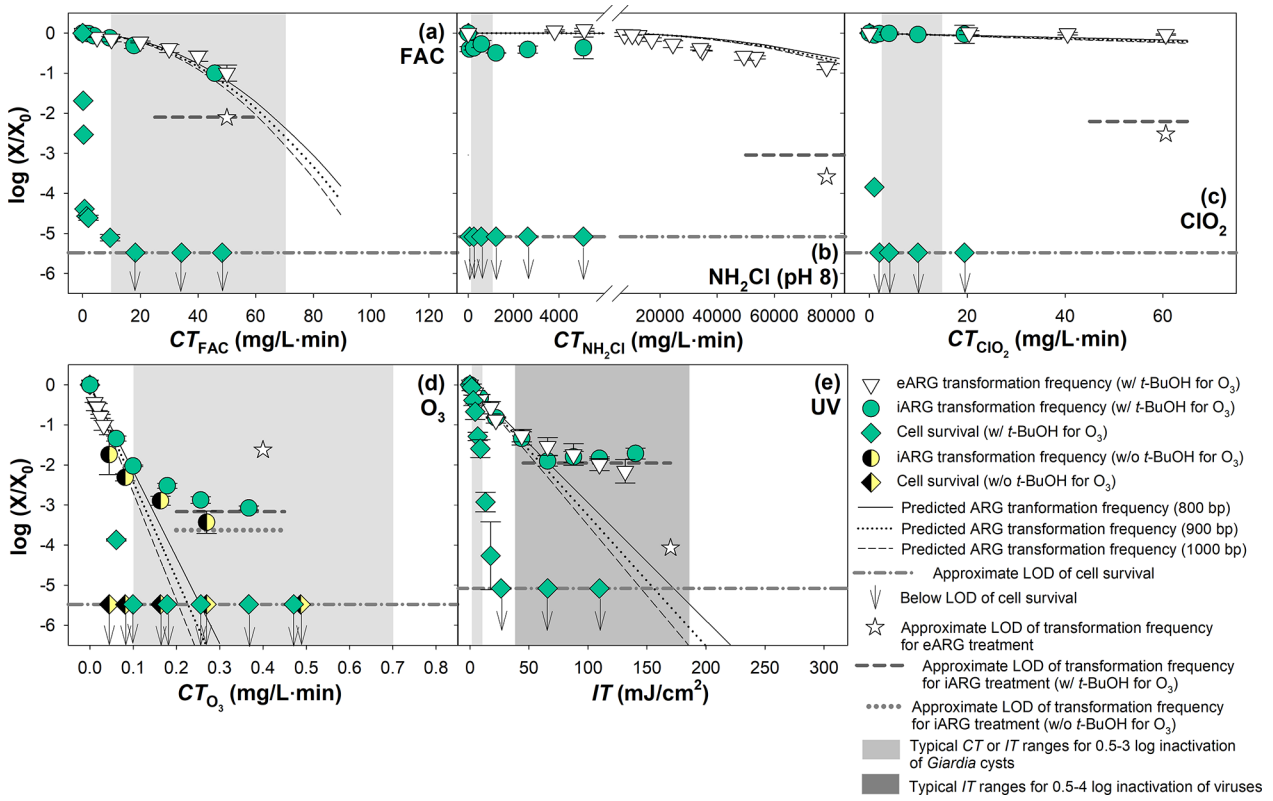

Figure 4. Normalized (log_{10}-scale) *measured* transformation frequency, cell survival, and *modeled* (predicted) transformation frequency (with the latter obtained using 800 bp, 900 bp, and 1000 bp homologous *acfA*-flanking sequences) versus disinfectant exposure for (a) FAC, (b) NH_2Cl, (c) ClO_2, (d) O_3, and (e) UV, during treatment of extracellular *B. subtilis* 1A189 DNA or intact *B. subtilis* 1A189 cells with each disinfectant in 10 mM phosphate buffer at pH 7 (FAC, ClO_2, O_3, and UV) or 8 (NH_2Cl only). Typical *CT* and *IT* ranges applied in drinking water practice when using each disinfectant to inactivate *Giardia* cysts[83] or viruses[84] are indicated by light gray-shaded and dark gray-shaded areas, respectively. Kinetics-based predictions of transformation frequency losses were obtained using the model in SI Text S9 for FAC and NH_2Cl, eq 7 for ClO_2 and O_3, and eq 8 for UV, where theoretical *degradation* rate constants, $k_{Disinfectant,\ Amp}$, for the 800 bp, 900 bp ,and 1000 bp homologous *acfA*-flanking sequences (Scheme 1, SI Text S5) were calculated by means of eq 9, using the values of $k_{Disinfectant,\ Specific}$ and $k_{Disinfectant,\ 0}$ provided in Table 1, and specific nucleotide contents of the homologous sequences (SI Table S1). The relatively high LOD for transformation frequency during UV treatment of iARGs is attributable to the lower total sample volume treated in UV experiments (100 mL) compared to other iARG experiments (1 L), which resulted in a lower sample preconcentration factor during the workup for analyses in the UV experiments. Error bars (representing one standard deviation from the mean) for transformation frequency and cell survival were obtained from duplicate experiments conducted independently, except that cell viabilities for (c) ClO_2 were only measured for one of the duplicate experiments (and are thus shown without error bars).

minimum length of homology (~400−500 bp) is required on each side of a nonhomologous sequence (here a point mutation, *acfA*, so ~800−1000 bp in total) for successful natural transformation in *B. subtilis*, in analogy with requirements observed for various other bacterial species.[72,73] Damage within the requisite homologous flanking sequence would be anticipated to disable or hinder transformation. It has also been shown that a decrease in donor DNA size from several kbps down to the minimum required length causes a continual decrease in transforming activity—potentially due to a decrease in attachment and/or donor−acceptor complexation efficiencies.[72,74]

For FAC, NH_2Cl, ClO_2, O_3, and UV, which attack DNA primarily through selective nucleotide modification without impacting DNA strand size (as confirmed by PFGE; SI Figure S18a−e), ARG transforming activity would not be diminished unless lesions occur within the ~800−1000 bp flanking region noted above. In an analogous manner, one or more lesions within the targeted amplicon would result in *detectable* loss of qPCR signals, while those outside would have no influence. If the monitored qPCR amplicon comprises either the homologous flanking region itself, or another region with similar nucleotide content at a different locus (even far from the flanking region), synchronization in the kinetics of amplicon *degradation* and ARG *deactivation* would therefore be expected. Here, the 832−1017 bp amplicons incur damage by FAC, NH_2Cl, ClO_2, O_3, and UV at similar rates as ARG *deactivation* (Figure 3a−e) because they have nucleotide contents similar to (but only partly overlapping with) the ~800−1000 bp homologous flanking sequences centered on the *acfA* mutation (Scheme 1, SI Text S5 and Table S1).

In contrast, $^{\bullet}OH$ damages DNA predominantly by strand fragmentation (via phosphate backbone cleavage), resulting in decreased DNA length and most likely diminished attachment and/or donor−acceptor complexation efficiencies with increasing exposure (SI Figure S18f).[75] Consequently, even if $^{\bullet}OH$ damages a DNA strand at a location outside of the requisite flanking region (or the region encompassed by the monitored amplicon), ARG transforming activity can be lowered due to a decrease in strand length, while monitored amplicons may remain undamaged, leading to consistently faster rates of ARG *deactivation* than amplicon *degradation* (Figures 1f and 3f).

DOI: 10.1021/acs.est.8b04393
Environ. Sci. Technol. 2019, 53, 2013−2026

The tailing in ARG *deactivation* by ClO_2 and UV (Figure 1c,e) and consequent deviation from 1:1 *degradation:deactivation* relationships (Figure 3c,e) may be partly due to dark-repair of lesions likely to result from ClO_2 or UV exposure − such as 8-oxoG[76] or TT-CPDs[26,77] − in damaged DNA upon uptake by the *B. subtilis* 1A1 recipient cells during transformation assays. Photorepair can be excluded since transformation assays were conducted with only brief exposures to indoor light (only during sample handling at room temperature, prior to/between incubations in the dark) and yielded results consistent with controls conducted fully in the dark (data not shown). For UV, the tailing effect (also observable to a lesser degree in qPCR results; SI Figure S14) may also be partly explained by CPD photoreversal at higher fluences.[55] Prior work has likewise demonstrated tailing in ARG *degradation*[27,29] and *deactivation*[25] profiles during UV irradiation.

The correlations of qPCR analyses with genomic ARG transforming activity measurements observed here may extend to a number of other bacteria. In addition to *Bacillus*, many other naturally competent bacterial genera—including important pathogens (e.g., *Haemophilus*,[78] *Streptococcus*,[79] *Neiserria*,[80] *Acinetobacter*[81])—exhibit minimum flanking homology requirements for natural transformation with genomic DNA, suggesting that *deactivation* of ARGs encoded within their genomes could likewise depend on damage to identifiable "critical sequences" of DNA. For cases involving plasmid transformation (not generally driven by homologous recombination), ARG *deactivation* appears less likely to correlate directly with qPCR measurements of ARG *degradation*.[27,60] In such cases, plasmids' origins of replication, which are critical to plasmid function, may represent an alternative target for tracking ARG activity loss.[60]

iARG *Deactivation* and ARB *Inactivation*. *Degradation* and *deactivation* of iARGs by each disinfectant was also investigated as a comparison to eARG results, and to evaluate the possible influence of cell constituents on ARG *degradation/deactivation*. Direct exposure of iARGs to $^{\bullet}OH$ was not included, as $^{\bullet}OH$ has previously been shown to have negligible effect on iARGs, even under conditions typical of advanced oxidation processes (e.g., UV/H_2O_2).[19]

As shown in Figure 4, iARG *deactivation* lagged ARB inactivation for all of the five disinfectants investigated. Analogous results were observed for iARG *degradation* (SI Figure S19), clearly demonstrating that iARGs may "survive" disinfection processes even if the associated ARB cells are effectively inactivated. Similar results have been reported in previous studies of iARG *degradation* by various disinfectants,[19,22,24,29] These findings can be explained by the fact that disinfectants often react with other vital cellular components (e.g., cell-envelope lipids or proteins, cellular enzymes, etc.) before reaching DNA within the cytoplasm, as for FAC, NH_2Cl, ClO_2, and O_3. In the case of UV, damage to the full bacterial genome that inhibits vital cellular functions likely accumulates much faster than damage to a much shorter ARG, leading to cell inactivation prior to measurable ARG damage.[82]

General consistency was found in the kinetics of iARG and eARG *deactivation* within investigated exposure ranges for each disinfectant, indicating that the cell envelope and other cellular biomolecules did not significantly hinder the ability of disinfectants to reach and react with the ARB cells' DNA. Only a marginal difference was observed between iARG *deactivation* by O_3 with and without *t*-BuOH (Figure 4d), suggesting a minimal role of $^{\bullet}OH$ due to its rapid scavenging by other intracellular components.[19] For UV (Figure 4e), iARG *deactivation* exhibited tailing similar to that observed during eARG *deactivation* (presumably for similar reasons as discussed above).

Differences were observed between iARG and eARG *deactivation* curves for NH_2Cl at CT_{NH2Cl} < 60 mg/L·min and O_3 at CT_{O3} > 0.1 mg/L·min. For NH_2Cl (Figure 4b), iARG transforming activity initially exhibited a rapid drop followed by minimal subsequent loss, whereas the four qPCR amplicons remained largely intact throughout the investigated exposure range (SI Figures S19b, S20b). This is analogous to trends observed in reaction of $^{\bullet}OH$ with eARGs (Figures 1f, 3f), and may have resulted from DNA fragmentation due to $^{\bullet}OH$ or Fe(IV) generation by NH_2Cl reactions with intracellular reduced metal ions (e.g., Fe^{2+}).[56,85] Although FAC is also known to be able to induce formation of such radicals under similar conditions,[56,85,86] FAC's reaction with iARGs may have been fast enough to outweigh radical contributions (in contrast with the exceptionally slow kinetics of NH_2Cl). For O_3 (Figure 4d), the evident tailing in iARG deactivation at higher exposures may be attributable to accelerated direct consumption and/or radical chain decomposition of O_3 within the vicinity of the cell envelope and/or cytoplasm of the *B. subtilis* 1A189 cells, due to increased solubilization of reactive biomolecules (e.g., cell-envelope amino acids or unsaturated lipids) during cell lysis.[82,87]

Implications for (Waste)Water Disinfection Practice. To facilitate comparison of experimental conditions with practical scenarios, eARG and iARG *deactivation* data in Figure 4 are overlain with exposure ranges likely to be encountered in (waste)water disinfection practice (conservatively based on drinking water disinfection requirements).[83,84] Analogous comparisons for ARG *degradation* are provided in SI Figure S19. Light gray-shaded areas in Figure 4a−e represent *CT*s or *IT*s required for 0.5−3-log_{10} inactivation of *Giardia* cysts at pH 7, 20 °C for each disinfectant.[83] The dark gray-shaded area in Figure 4e represents *IT*s required for 0.5−4-log_{10} inactivation of viruses by UV.[84] The *CT* and *IT* requirements for 2-log_{10} *deactivation* of eARGs and iARGs, and 2-log_{10} *degradation* of the four eARG amplicons (based on Figures 1 and 4), are also summarized with available literature values for each disinfectant in SI Table S3.

These comparisons indicate that FAC should be capable of achieving up to ∼2-log_{10} chromosomal ARG *deactivation* at practical CT_{FAC} ranges (Figure 4a), which is ∼2.5× less efficient than previously reported for plasmid-borne ARGs[19] (possibly due to differences in plasmid and genomic DNA reactivities toward FAC, as noted above). For O_3, up to ∼3-log_{10} ARG *deactivation* should be achievable at practical CT_{O3} ranges (Figure 4d), consistent with previous findings.[24] UV light would be anticipated to yield <0.5-log_{10} ARG *deactivation* at the upper end of the *IT* range for *Giardia* cysts, and ∼2-log_{10} *deactivation* within the *IT* range for viruses (Figure 4e). These observations are generally consistent with previous findings obtained under comparable conditions,[19,27,29,60] although lower UV efficiencies have also been reported.[28]

In contrast to FAC, O_3, and UV, NH_2Cl and ClO_2 were found to yield minimal ARG *deactivation* even at their highest practical *CT* levels for (waste)water treatment. Previous studies have also shown that NH_2Cl[20] and ClO_2[22,66,88] exhibit marginal reactivity toward bacterial DNA. For instance, NH_2Cl treatment at 37 °C was found to yield <0.8-log_{10} *deactivation* of

DOI: 10.1021/acs.est.8b04393
Environ. Sci. Technol. 2019, 53, 2013−2026

extracellular *B. subtilis* DNA at a CT_{NH2Cl} up to ~4000 mg/L·min, and ~0.7-log_{10} *deactivation* for intracellular *B. subtilis* DNA at a CT_{NH2Cl} of ~170 mg/L·min[20] (also consistent with the differences in levels of iARG and eARG *deactivation* observed here at lower NH_2Cl exposures). For ClO_2, *deactivation* of an eARG of *H. influenzae* DNA was moderately faster than observed here, but a CT_{ClO2} of ~75 mg/L·min still only yielded <1-log_{10} *deactivation*.[22] These results highlight the wide variations in abilities of different disinfectants to degrade/deactivate ARGs at practical *CT* or *IT* ranges.

It is also important to note that applications of O_3 and UV may frequently be based on more or less conservative criteria than disinfection requirements. For example, O_3 exposures targeting micropollutant elimination have been shown to yield inefficient ARG *degradation*.[24] In contrast, UV fluences applied in UV/H_2O_2 processes—likely to be greater than even the highest *IT*s required for virus inactivation (Figure 4e),[89,90] have been reported to yield ≥2-log_{10} ARG *degradation*.[19] Furthermore, application of FAC for achieving pathogen inactivation during wastewater disinfection is likely to be ineffective for ARG *degradation/deactivation* under typical conditions, as FAC would be converted almost instantaneously to nonreactive NH_2Cl in non-nitrified wastewaters unless breakpoint chlorination is practiced.[91]

The influence of water quality parameters (e.g., dissolved organic matter, turbidity, pH) and susceptibilities of ARGs (plasmid-borne and genomic) from a wider variety of bacterial species should also be evaluated further to more fully assess the practical performance of each disinfectant.

qPCR and Kinetics-Based Models for Predicting Elimination of ARG Biological Activity. The results depicted in Figures 3, 4, and SI Figures S19, S20 suggest that in addition to direct qPCR analyses of a "critical sequence" required for natural transformation of an ARG, qPCR analyses *of any other alternative sequence on the bacterial chromosome with a nucleotide content equivalent to the critical sequence* could be used to detect DNA damage at a rate equivalent to ARG *deactivation*. It is also possible that qPCR analyses of such *alternative* sequences could be used to detect damage to other important chromosomally encoded genes (e.g., virulence factors) as an indication of their transforming activities. This concept has parallels in the use of qPCR to monitor losses of viral infectivity[92] and bacterial plasmid transforming activity during UV irradiation.[27] The potential to target such *alternative* sequence(s) presents an attractive option for qPCR assays, as it is sometimes difficult to reliably amplify a desired DNA region due to issues such as primer dimerization or nonspecific amplification.

Furthermore, the clear dependence of qPCR amplicon *degradation* kinetics on contents of certain bps or doublets (Figure 2, Table 1, and associated discussion) suggests that under certain circumstances, it may be possible to predict the kinetics of ARG *degradation* (and hence, ARG *deactivation*) by a disinfectant based on knowledge of the sequences of the ARG and its flanking regions (or other "critical sequence(s)"), coupled with appropriate *sequence-independent* rate constants (Table 1). As a demonstration of this, an envelope of theoretical ARG *deactivation* curves was modeled according to SI Text S9 for FAC and NH_2Cl, eq 7 for ClO_2 and O_3, and eq 8 for UV, by predicting theoretical *degradation* rate constants, $k_{Disinfectant, Amp}$, for the 800 bp, 900 bp, and 1000 bp homologous flanking sequences centered on the *acfA* mutation in *B. subtilis* 1A189 DNA (Scheme 1, SI Text S5) with eq 9, using their nucleotide contents (SI Table S1) and the sequence-independent rate constants $k_{Disinfectant, Specific}$ and $k_{Disinfectant, 0}$ for FAC, NH_2Cl, ClO_2, O_3, or UV (Table 1). As shown in Figure 4, the resulting model predictions generally agreed well with measured results for *deactivation* of eARGs and iARGs up to exposures sufficient to yield roughly 1−2 log_{10} *deactivation*. The overall good predictions (Figure 4), along with the strong *degradation:deactivation* correlations in Figure 3, suggest that such models may prove useful as a generally applicable means for predicting ARG *degradation and deactivation* during treatment with these five disinfectants.

Based on the findings reported here and in previous work, it appears that qPCR analyses and kinetics-based model predictions have the potential to be employed as surrogates for ARG *deactivation* when "critical sequences" required for transformation of genomic or plasmid-borne ARGs can be identified. However, such approaches should be applied with caution. As discussed above, significant tailing in ARG *deactivation* curves was noted during treatment of iARGs and/or eARGs with ClO_2, O_3, and UV at high exposures (Figures 1c,e and 4d,e). In such cases, qPCR-based approximations or kinetics-based predictions of ARG *deactivation* could result in overestimation of actual *deactivation* levels. Additional work will be required to determine how generally these findings apply to different ARGs and bacterial species.

■ ASSOCIATED CONTENT

Supporting Information

The Supporting Information is available free of charge on the ACS Publications website at DOI: 10.1021/acs.est.8b04393.

Definitions of acronyms and symbols; texts, tables, and figures addressing detailed procedures of DNA extraction, DNA analyses (including transformation assay, qPCR assays, and PFGE), and disinfection experiments; ARG and primer sequences and nucleotide contents; determinations of reaction kinetics and rate constants for each disinfectant; detailed discussions of FAC and NH_2Cl reaction kinetics, mechanisms, and associated kinetic model development; estimates of theoretical diffusion-controlled rate constants for $^{\bullet}OH$; comparisons of rate constants from the present work with literature values; PFGE results for each disinfectant; and ARG *degradation* during iARG experiments (SI Part A) (PDF)

Kinetic models for FAC and NH_2Cl reactions; weighted linear regressions of $k_{Disinfectant, Amp}$ versus molar contents of various nucleotide *bps*, doublets, and triplets for each of the 266−1017 bp amplicons (SI Parts B−D; in Excel format) (ZIP)

■ AUTHOR INFORMATION

Corresponding Author

*Phone: 206-685-7583; fax: 206-543-1543; e-mail: doddm@uw.edu.

ORCID

Kyle K. Shimabuku: 0000-0001-8497-5945
Yunho Lee: 0000-0001-5923-4897
Michael C. Dodd: 0000-0001-7544-1642

Author Contributions

§P.Z. and K.S. contributed equally to this work.

DOI: 10.1021/acs.est.8b04393
Environ. Sci. Technol. 2019, 53, 2013−2026

Notes

The authors declare no competing financial interest.

■ ACKNOWLEDGMENTS

This material is based upon work supported by the National Science Foundation under Grant Number CBET-1254929. Dr. Daniel R. Zeigler (BGSC), Dr. Heidi Gough, Dr. J. Scott Meschke, Dr. Nicolette Zhou, and statistics tutors at the UW Statistics Tutor & Study Center are greatly acknowledged for their technical support and advice. Three anonymous reviewers are gratefully acknowledged for their insightful and helpful comments, which have greatly strengthened this work.

■ REFERENCES

(1) Davies, J.; Davies, D. Origins and Evolution of Antibiotic Resistance. *Microbiol. Mol. Biol. Rev.* **2010**, *74* (3), 417−433.
(2) *Antibiotic Resistance Theats in the United States, 2013*; U.S. Department of Health and Human Services Centers for Disease Control and Prevention, 2013.
(3) Roberts, R. R.; Hota, B.; Ahmad, I.; Scott, R. D.; Foster, S. D.; Abbasi, F.; Schabowski, S.; Kampe, L. M.; Ciavarella, G. G.; Supino, M.; Naples, J.; Cordell, R.; Levy, S. B.; Weinstein, R. A. Hospital and Societal Costs of Antimicrobial-Resistant Infections in a Chicago Teaching Hospital: Implications for Antibiotic Stewardship. *Clin. Infect. Dis.* **2009**, *49* (8), 1175−1184.
(4) Pruden, A.; Pei, R. T.; Storteboom, H.; Carlson, K. H. Antibiotic resistance genes as emerging contaminants: Studies in northern Colorado. *Environ. Sci. Technol.* **2006**, *40* (23), 7445−7450.
(5) McKinney, C. W.; Loftin, K. A.; Meyer, M. T.; Davis, J. G.; Pruden, A. tet and sul Antibiotic Resistance Genes in Livestock Lagoons of Various Operation Type, Configuration and Antibiotic Occurrence. *Environ. Sci. Technol.* **2010**, *44* (16), 6102−6109.
(6) Czekalski, N.; Berthold, T.; Caucci, S.; Egli, A.; Buergmann, H. Increased levels of multiresistant bacteria and resistance genes after wastewater treatment and their dissemination into Lake Geneva, Switzerland. *Front. Microbiol.* **2012**, DOI: 10.3389/fmicb.2012.00106.
(7) Ma, Y. J.; Wilson, C. A.; Novak, J. T.; Riffat, R.; Aynur, S.; Murthy, S.; Pruden, A. Effect of Various Sludge Digestion Conditions on Sulfonamide, Macrolide, and Tetracycline Resistance Genes and Class I Integrons. *Environ. Sci. Technol.* **2011**, *45* (18), 7855−7861.
(8) Luo, Y.; Yang, F.; Mathieu, J.; Mao, D.; Wang, Q.; Alvarez, P. J. J. Proliferation of Multidrug-Resistant New Delhi Metallo-β-lactamase Genes in Municipal Wastewater Treatment Plants in Northern China. *Environ. Sci. Technol. Lett.* **2014**, *1* (1), 26−30.
(9) Pei, R. T.; Kim, S. C.; Carlson, K. H.; Pruden, A. Effect of River Landscape on the sediment concentrations of antibiotics and corresponding antibiotic resistance genes (ARG). *Water Res.* **2006**, *40* (12), 2427−2435.
(10) Xi, C. W.; Zhang, Y. L.; Marrs, C. F.; Ye, W.; Simon, C.; Foxman, B.; Nriagu, J. Prevalence of Antibiotic Resistance in Drinking Water Treatment and Distribution Systems. *Appl. Environ. Microbiol.* **2009**, *75* (17), 5714−5718.
(11) Ma, L.; Li, B.; Jiang, X.-T.; Wang, Y.-L.; Xia, Y.; Li, A.-D.; Zhang, T. Catalogue of antibiotic resistome and host-tracking in drinking water deciphered by a large scale survey. *Microbiome* **2017**, *5* (1), 154.
(12) Levy, S. B.; Miller, R. V. *Gene transfer in the environment*; McGraw-Hill, Inc.: New York, NY, 1994.
(13) Lorenz, M. G.; Wackernagel, W. Bacterial gene transfer by natural genetic transformation in the environment. *Microbiol. Rev.* **1994**, *58* (3), 563−602.
(14) Johnsborg, O.; Eldholm, V.; Havarstein, L. S. Natural genetic transformation: prevalence, mechanisms and function. *Res. Microbiol.* **2007**, *158* (10), 767−778.
(15) *Pathogen Safety Data Sheets and Risk Assessment*; Public Health Agency of Canada, 2012, http://www.phac-aspc.gc.ca/lab-bio/res/psds-ftss/index-eng.php#e.
(16) Domingues, S.; Harms, K.; Fricke, W. F.; Johnsen, P. J.; da Silva, G. J.; Nielsen, K. M. Natural Transformation Facilitates Transfer of Transposons, Integrons and Gene Cassettes between Bacterial Species. *PLoS Pathog.* **2012**, *8*, e1002837.
(17) Lu, N.; Zilles, J. L.; Nguyen, T. H. Adsorption of Extracellular Chromosomal DNA and Its Effects on Natural Transformation of Azotobacter vinelandii. *Appl. Environ. Microbiol.* **2010**, *76* (13), 4179−4184.
(18) Cai, P.; Huang, Q. Y.; Zhang, X. W. Interactions of DNA with clay minerals and soil colloidal particles and protection against degradation by DNase. *Environ. Sci. Technol.* **2006**, *40* (9), 2971−2976.
(19) Yoon, Y.; Chung, H. J.; Di, D. Y. W.; Dodd, M. C.; Hur, H.-G.; Lee, Y. Inactivation efficiency of plasmid-encoded antibiotic resistance genes during water treatment with chlorine, UV, and UV/H2O2. *Water Res.* **2017**, *123*, 783−793.
(20) Shih, K. L.; Lederberg, J. Effects of chloramine on *Bacillus subtilis* deoxyribonucleic acid. *J. Bacteriol.* **1976**, *125* (3), 934−945.
(21) Guo, M.-T.; Yuan, Q.-B.; Yang, J. Distinguishing effects of ultraviolet exposure and chlorination on the horizontal transfer of antibiotic resistance genes in municipal wastewater. *Environ. Sci. Technol.* **2015**, *49* (9), 5771−5778.
(22) Roller, S. D.; Olivieri, V. P.; Kawata, K. Mode of bacterial inactivation by chlorine dioxide. *Water Res.* **1980**, *14* (6), 635−641.
(23) Hamelin, C. Production of Single- and Double-strand Breaks in Plasmid DNA by Ozone. *Int. J. Radiat. Oncol., Biol., Phys.* **1985**, *11* (2), 253−257.
(24) Czekalski, N.; Imminger, S.; Salhi, E.; Veljkovic, M.; Kleffel, K.; Drissner, D.; Hammes, F.; Bürgmann, H.; Von Gunten, U. Inactivation of antibiotic resistant bacteria and resistance genes by ozone: from laboratory experiments to full-scale wastewater treatment. *Environ. Sci. Technol.* **2016**, *50* (21), 11862−11871.
(25) Lerman, L. S.; Tolmach, L. J. Genetic transformation. 2. The significance of damage to the DNA molecule. *Biochim. Biophys. Acta* **1959**, *33* (2), 371−387.
(26) Setlow, J. K. Shape of UV inactivation curve for transforming DNA. *Nature* **1977**, *268* (5616), 169−170.
(27) Chang, P. H.; Juhrend, B.; Olson, T. M.; Marrs, C. F.; Wigginton, K. R. Degradation of extracellular antibiotic resistance genes with UV254 treatment. *Environ. Sci. Technol.* **2017**, *51* (11), 6185−6192.
(28) Destiani, R.; Templeton, M. R.; Kowalski, W. Relative Ultraviolet Sensitivity of Selected Antibiotic Resistance Genes in Waterborne Bacteria. *Environ. Eng. Sci.* **2017**, *35* (7), 770−774.
(29) McKinney, C. W.; Pruden, A. Ultraviolet disinfection of antibiotic resistant bacteria and their antibiotic resistance genes in water and wastewater. *Environ. Sci. Technol.* **2012**, *46* (24), 13393−13400.
(30) Markham, P. N.; Neyfakh, A. A. Efflux-mediated drug resistance in Gram-positive bacteria. *Curr. Opin. Microbiol.* **2001**, *4* (5), 509−514.
(31) Poole, K. Efflux-mediated antimicrobial resistance. *J. Antimicrob. Chemother.* **2005**, *56* (1), 20−51.
(32) Fluman, N.; Bibi, E. Bacterial multidrug transport through the lens of the major facilitator superfamily. *Biochim. Biophys. Acta, Proteins Proteomics* **2009**, *1794* (5), 738−747.
(33) Earl, A. M.; Losick, R.; Kolter, R. Ecology and genomics of Bacillus subtilis. *Trends Microbiol.* **2008**, *16* (6), 269−275.
(34) Ahmed, M.; Lyass, L.; Markham, P. N.; Taylor, S. S.; Vazquezlaslop, N.; Neyfakh, A. A. Two highly similar multidrug transporters of *Bacillus subtilis* whose expression is differentially regulated. *J. Bacteriol.* **1995**, *177* (14), 3904−3910.
(35) Saito, H.; Miura, K. Preparation of transforming deoxyribonucleic acid by phenol treatment. *Biochim. Biophys. Acta, Spec. Sect. Nucleic Acids Relat. Subj.* **1963**, *72* (4), 619−629.
(36) Bott, K. F.; Wilson, G. A. Development of competence in *Bacillus subtilis* transformation system. *J. Bacteriol.* **1967**, *94* (3), 562−570.

DOI: 10.1021/acs.est.8b04393
Environ. Sci. Technol. 2019, 53, 2013−2026

(37) Anagnostopoulos, C.; Spizizen, J. Requirements for transformation in *Bacillus subtilis*. *J. Bacteriol.* **1961**, *81* (5), 741.
(38) Shimelis, O.; Giese, R. W. Nuclease P1 digestion/high-performance liquid chromatography, a practical method for DNA quantitation. *J. Chromatogr. A* **2006**, *1117* (2), 132−136.
(39) Dodd, M. C.; Vu, N. V.; Le, V. C.; Kissner, R.; Pham, H. V.; Cao, T. H.; Berg, M.; von Gunten, U. Kinetics and mechanistic aspects of As(III) oxidation by aqueous chlorine, chloramines, and ozone: Relevance to drinking water treatment. *Environ. Sci. Technol.* **2006**, *40* (10), 3285−3292.
(40) APHA *Standard Methods for the Examination of Water and Wastewater*, 21 ed.; APHA, AWWA, WPCF, 2005.
(41) Pinkernell, U.; Nowack, B.; Gallard, H.; Von Gunten, U. Methods for the photometric determination of reactive bromine and chlorine species with ABTS. *Water Res.* **2000**, *34* (18), 4343−4350.
(42) Bader, H.; Hoigné, J. Determination of ozone in water by the indigo method. *Water Res.* **1981**, *15* (4), 449−456.
(43) Canonica, S.; Meunier, L.; Von Gunten, U. Phototransformation of selected pharmaceuticals during UV treatment of drinking water. *Water Res.* **2008**, *42*, 121−128.
(44) Bolton, J. R.; Stefan, M. I.; Shaw, P.-S.; Lykke, K. R. Determination of the quantum yields of the potassium ferrioxalate and potassium iodide−iodate actinometers and a method for the calibration of radiometer detectors. *J. Photochem. Photobiol. A* **2011**, *222*, 166−169.
(45) Zepp, R. G. Quantum yields for reaction of pollutants in dilute aqueous solution. *Environ. Sci. Technol.* **1978**, *12* (3), 327−329.
(46) Elovitz, M. S.; von Gunten, U. Hydroxyl radical/ozone ratios during ozonation processes. I. The Rct concept. *Ozone: Sci. Eng.* **1999**, *21* (3), 239−260.
(47) Shioi, J.; Matsuura, S.; Imae, Y. Quantitative measurements of proton motive force and motility in Bacillus subtilis. *J. Bacteriol.* **1980**, *144* (3), 891−897.
(48) Beck, N.; Callahan, K.; Nappier, S.; Kim, H.; Sobsey, M.; Meschke, J. Development of a spot-titer culture assay for quantifying bacteria and viral indicators. *J. Rapid Methods Autom. Microbiol.* **2009**, *17* (4), 455−464.
(49) Miller, J.; Miller, J. C. *Statistics and chemometrics for analytical chemistry*; Pearson Education, 2018.
(50) Ayala-Torres, S.; Chen, Y. M.; Svoboda, T.; Rosenblatt, J.; Van Houten, B. Analysis of gene-specific DNA damage and repair using quantitative polymerase chain reaction. *Methods* **2000**, *22* (2), 135−147.
(51) Sikorsky, J. A.; Primerano, D. A.; Fenger, T. W.; Denvir, J. Effect of DNA damage on PCR amplification efficiency with the relative threshold cycle method. *Biochem. Biophys. Res. Commun.* **2004**, *323*, 823−830.
(52) Duigou, S.; Ehrlich, S. D.; Noirot, P.; Noirot-Gros, M. F. DNA polymerase I acts in translesion synthesis mediated by the Y-polymerases in Bacillus subtilis. *Mol. Microbiol.* **2005**, *57* (3), 678−690.
(53) Filaderli, H. A. *Chlorination of Specific Organic Compounds in Water Treatment*; Department of Civil Engineering, Imperial College, 1989.
(54) Evans, M. D.; Cooke, M. S. *Oxidative Damage to Nucleic Acids*; Springer Science & Business Media, 2007.
(55) Law, Y. K.; Forties, R. A.; Liu, X.; Poirier, M. G.; Kohler, B. Sequence-dependent thymine dimer formation and photoreversal rates in double-stranded DNA. *Photochem. Photobiol. Sci.* **2013**, *12* (8), 1431−1439.
(56) Prutz, W. A. Hypochlorous acid interactions with thiols, nucleotides, DNA, and other biological substrates. *Arch. Biochem. Biophys.* **1996**, *332* (1), 110−120.
(57) Theruvathu, J. A.; Flyunt, R.; Aravindakumar, C. T.; von Sonntag, C. Rate constants of ozone reactions with DNA, its constituents, and related compounds. *J. Chem. Soc., Perkin Trans.* **2001**, *2* (3), 269−274.
(58) Masuda, T.; Shinohara, H.; Eda, M.; Kondo, M. Reactivity of nucleotides and polynucleotides toward hydroxyl radical in aqueous solution. *J. Radiat. Res.* **1980**, *21* (2), 173−179.
(59) Udovičić, L.; Mark, F.; Bothe, E. Yields of single-strand breaks in double-stranded calf thymus DNA irradiated in aqueous solution in the presence of oxygen and scavengers. *Radiat. Res.* **1994**, *140* (2), 166−171.
(60) Yoon, Y.; Dodd, M. C.; Lee, Y. Elimination of transforming activity and gene degradation during UV and UV/H2O2 treatment of plasmid-encoded antibiotic resistance genes. *Environ. Sci.: Water Res. Technol.* **2018**, *4*, 1239−1251.
(61) Patrick, M. H. Studies on Thymine-derived UV photoproducts in DNA —I. Formation and Biological Role of Pyrimidine Adducts in DNA. *Photochem. Photobiol.* **1977**, *25* (4), 357−372.
(62) Douki, T. Low ionic strength reduces cytosine photoreactivity in UVC-irradiated isolated DNA. *Photochem. Photobiol. Sci.* **2006**, *5* (11), 1045−1051.
(63) Tataurov, A. V.; You, Y.; Owczarzy, R. Predicting ultraviolet spectrum of single stranded and double stranded deoxyribonucleic acids. *Biophys. Chem.* **2008**, *133* (1-3), 66−70.
(64) Buxton, G. V.; Greenstock, C. L.; Helman, W. P.; Ross, A. B. Critical review of rate constants for reactions of hydrated electrons, hydrogen atoms and hydroxyl radicals (·OH/·O− in aqueous solution. *J. Phys. Chem. Ref. Data* **1988**, *17* (2), 513−886.
(65) von Sonntag, C. *Free-Radical-Induced DNA Damage and Its Repair*; Springer, 2006.
(66) Napolitano, M. J.; Stewart, D. J.; Margerum, D. W. Chlorine dioxide oxidation of guanosine 5′-monophosphate. *Chem. Res. Toxicol.* **2006**, *19* (11), 1451−1458.
(67) Sugiyama, H.; Saito, I. Theoretical studies of GG-specific photocleavage of DNA via electron transfer: significant lowering of ionization potential and 5 ‘-localization of HOMO of stacked GG bases in B-Form DNA. *J. Am. Chem. Soc.* **1996**, *118* (30), 7063−7068.
(68) Fukuzumi, S.; Miyao, H.; Ohkubo, K.; Suenobu, T. Electron-transfer oxidation properties of DNA bases and DNA oligomers. *J. Phys. Chem. A* **2005**, *109* (15), 3285−3294.
(69) Sivey, J. D.; McCullough, C. E.; Roberts, A. L. Chlorine monoxide (Cl2O) and molecular chlorine (Cl2) as active chlorinating agents in reaction of dimethenamid with aqueous free chlorine. *Environ. Sci. Technol.* **2010**, *44* (9), 3357−3362.
(70) Sivey, J. D.; Roberts, A. L. Assessing the reactivity of free chlorine constituents Cl2, Cl2O, and HOCl toward aromatic ethers. *Environ. Sci. Technol.* **2012**, *46* (4), 2141−2147.
(71) Vikesland, P. J.; Pruden, A.; Alvarez, P. J.; Aga, D.; Bürgmann, H.; Li, X.-d.; Manaia, C. M.; Nambi, I.; Wigginton, K.; Zhang, T. Toward a Comprehensive Strategy to Mitigate Dissemination of Environmental Sources of Antibiotic Resistance. *Environ. Sci. Technol.* **2017**, *51* (22), 13061−13069.
(72) Dubnau, D., Genetic exchange and homologous recombination. In *Bacillus subtilis and Other Gram-Positive Bacteria: Biochemistry, Physiology, And Molecular Genetics*; Sonenshein, A. L., Hoch, J. A., Losick, R., Eds.; American Society for Microbiology: Washington DC, 1993; pp 555−584.
(73) Contente, S.; Dubnau, D. Marker rescue transformation by linear plasmid DNA in Bacillus subtilis. *Plasmid* **1979**, *2* (4), 555−571.
(74) Morrison, D. A.; Guild, W. R. Activity of deoxyribonucleic acid fragments of defined size in *Bacillus subtilis* transformation. *J. Bacteriol.* **1972**, *112* (1), 220−223.
(75) Balasubramanian, B.; Pogozelski, W. K.; Tullius, T. D. DNA strand breaking by the hydroxyl radical is governed by the accessible surface areas of the hydrogen atoms of the DNA backbone. *Proc. Natl. Acad. Sci. U. S. A.* **1998**, *95* (17), 9738−9743.
(76) David, S. S.; O’shea, V. L.; Kundu, S. Base-excision repair of oxidative DNA damage. *Nature* **2007**, *447* (7147), 941.
(77) Hadden, C. T. Postreplication repair of ultraviolet-irradiated transforming deoxyribonucleic acid in *Bacillus subtilis*. *J. Bacteriol.* **1981**, *145* (1), 434−441.

DOI: 10.1021/acs.est.8b04393
Environ. Sci. Technol. 2019, 53, 2013−2026

(78) Herbert, M. A.; Hood, D. W.; Moxon, E. R. *Haemophilus Influenzae Protocols*; Springer Science & Business Media, 2003.
(79) Hakenbeck, R.; Chhatwal, S. *Molecular Biology of Streptococci*; Horizon Scientific Press, 2007.
(80) Hamilton, H. L.; Dillard, J. P. Natural transformation of Neisseria gonorrhoeae: from DNA donation to homologous recombination. *Mol. Microbiol.* **2006**, *59* (2), 376−385.
(81) Simpson, D. J.; Dawson, L. F.; Fry, J. C.; Rogers, H. J.; Day, M. J. Influence of flanking homology and insert size on the transformation frequency of Acinetobacter baylyi BD413. *Environ. Biosaf. Res.* **2007**, *6* (1−2), 55−69.
(82) Dodd, M. C. Potential impacts of disinfection processes on elimination and deactivation of antibiotic resistance genes during water and wastewater treatment. *J. Environ. Monit.* **2012**, *14*, 1754−1771.
(83) EPA. *Disinfection Profiling and Benchmarking Guidance Manual*; United States Environmental Protection Agency: Office of Water: Washington, DC, 1999.
(84) *Ultraviolet Disinfection Guidance Manual for the Final Long Term 2 Enhanced Surface Water Treatment Rule*; United States Environmental Protection Agency: Office of Water: Washington, DC, 2006.
(85) Imlay, J. A. Pathways of oxidative damage. *Annu. Rev. Microbiol.* **2003**, *57* (1), 395−418.
(86) Hawkins, C. L.; Davies, M. J. Hypochlorite-induced damage to DNA, RNA, and polynucleotides: formation of chloramines and nitrogen-centered radicals. *Chem. Res. Toxicol.* **2002**, *15* (1), 83−92.
(87) Manterola, G.; Uriarte, I.; Sancho, L. The effect of operational parameters of the process of sludge ozonation on the solubilisation of organic and nitrogenous compounds. *Water Res.* **2008**, *42* (12), 3191−3197.
(88) Hauchman, F. S.; Noss, C. I.; Olivieri, V. P. Chlorine dioxide reactivity with nucleic acids. *Water Res.* **1986**, *20* (3), 357−361.
(89) Lee, Y.; Gerrity, D.; Lee, M.; Gamage, S.; Pisarenko, A.; Trenholm, R. A.; Canonica, S.; Snyder, S. A.; Von Gunten, U. Organic contaminant abatement in reclaimed water by UV/H2O2 and a combined process consisting of O3/H2O2 followed by UV/H2O2: prediction of abatement efficiency, energy consumption, and byproduct formation. *Environ. Sci. Technol.* **2016**, *50* (7), 3809−3819.
(90) Rosenfeldt, E. J.; Linden, K. G.; Canonica, S.; Von Gunten, U. Comparison of the efficiency of OH radical formation during ozonation and the advanced oxidation processes O3/H2O2 and UV/H2O2. *Water Res.* **2006**, *40* (20), 3695−3704.
(91) Leong, L. Y. C.; Kuo, J.; Tang, C.-C. *Disinfection of Wastewater Effluent - Comparison of Alternative Technologies*; Water Environment Research Foundation: Alexandria, VA, 2008.
(92) Pecson, B. M.; Ackermann, M.; Kohn, T. Framework for Using Quantitative PCR as a Nonculture Based Method To Estimate Virus Infectivity. *Environ. Sci. Technol.* **2011**, *45* (6), 2257−2263.

DOI: 10.1021/acs.est.8b04393
Environ. Sci. Technol. 2019, 53, 2013−2026